

Analysis of Mesostructures along Jarash- Irbid Highway, Northern Jordan

Abdullah Diabat^{*1}, Tahreer Assaqir², Najmeddin Yusuf³, Muhammad Atallah⁴

¹Al al-Bayt University, Institute of Earth and Environmental Sciences, Department of Applied Earth and Environmental Sciences, Al al-Bayt University, Jordan

^{2,3,4}Yarmouk University, Faculty of Sciences, Department of earth and environmental sciences, Jordan

Received 26 January 2020; Accepted 29 March 2020

Abstract

Geologic structural surveys were conducted in many road cuts and quarries along the Irbid-Jarash highway, north of Thughart Asfour village. Meso-scale tectonic structures which were found in these stations including: folds, faults (Strike-slip, normal and reverse), joints, flower structures, boudinage structures and shear fractures, revealed that the area has undergone a local tensional as well as compressional stresses related to the regional one. More than 1385 fracture measurements were done using scanline, circle, and common methods in order to investigate the orientation and density of the fractures in different parts of the study area. Two dominant trends of joint sets (N-S and NNW to NW) and other minor trends (E-W, ENE-WSW and WNW-ESE) were found in the Cretaceous carbonate rocks (Wadi Es Sir Limestone Formation). The dominant trend sets represent the range of conjugated, hybrid, and extensional fractures in which the acute bisector of these represents the main trend of extensional fracture set, which in turn is consistency with the SHmax (maximum horizontal compressive stress axis) oriented NNW-SSE. Geometries of fractures in the carbonate rocks represent a continuum of structures at various stages of development that can be classified into two main geometric categories corresponding to increasing levels of brittle strain; bed- confined fractures and throughgoing fractures. Many throughgoing fractures develop subsequent to bed-confined joints by the coalescence of pre-existing joints. The spatial distribution of throughgoing fractures varies as a function of structural position. The highest frequency and estimated strain intensity have been located at the fold crests and fault zones.

© 2020 Jordan Journal of Earth and Environmental Sciences. All rights reserved

Keywords: Mesostructures, Throughgoing fractures, Bed-confined joints, Wadi Es Sir Limestone Formation, Northern Jordan.

1. Introduction

Mesostructures or mesoscopic structures range in size from one centimeter to a few meters and include small faults, small folds, stylolites, cleavages, shear zones, veins, and joints (Hancock, 1985). In many studies of deformed rocks, the presence of mesostructures has provided a useful tool for analyzing the stress and strain patterns in host or regional structures (Hancock and Atiyya, 1979; Eyal and Reches, 1983; Eyal et al., 2001).

The study of mesoscopic structures helps in strain analysis, provides information that can help in the interpretation of regional structural relations, and can provide clues about deformation conditions and sense of movement during deformation. The development of mesofracture sets and systems, that are symmetrically-oriented about sedimentary layers and hinge lines, leads to a shortening or an elongation parallel to or normal for those directions (Hancock, 1985). Fracture density can be measured and described in a number of ways, namely total cumulative length of fracture within a given volume of rock divided by area of the circle. The

measurement of fracture density used in conjunction with the circle inventory method is the summed length of all fractures within an inventory circles, divided by the area of the circle (Davis et al., 2011).

Eyal and Reches (1983) analyzed the mesostructures in Northern Palestine and found evidence from the mesostructures to support the hypothesis of strike-slip movement along the Dead Sea Transform. In Jordan, few detailed studies were carried out concerning mesostructures (e.g., Atallah, 1996; Al-Taj et al., 2003; Diabat et al., 2004; Diabat, 2009; Diabat, 2013; Radaideh and Melichar, 2015; Al-Awabdeh et al., 2016). Other areas in Jordan except for the DST fault have received little attention of tectonic and/or structural studies. The area upon which this study is focused is one of these poorly-investigated areas in Jordan. The study area is located few kilometers to the north of Jarash city and is bounded by the coordinates: 32° 19' & 32° 23' N and 35° 54' & 35° 56' E (Figure 1). The field covered in this study extends along the Jerash- Irbid Highway, north of Thughrat Asfour village, where numerous mesostructures can be observed in

* Corresponding author e-mail: adiabat@aabu.edu.jo

road-cut exposures and quarries of Wadi Es Sir Limestone Formation providing an excellent opportunity to investigate the kinematics related to their development.

The aim of this study is to increase knowledge about the various structures, and get better resolution of the bed-confined fractures and throughgoing fractures of the study area.

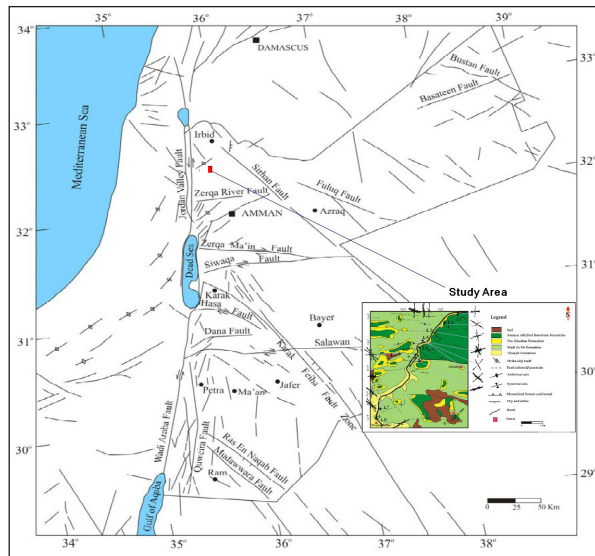


Figure 1. Structural pattern of Jordan and location of the study area (modified after Diabat and Masri, 2005).

2. Geological Setting

2.1. Stratigraphy

2.1.1. Ajloun Group

2.1.1.1. Shuayb Formation

The formation which conformably overlies the Hummar Formation consists mainly of yellow to yellow gray, thin- to medium-bedded marly limestone, nodular limestone, and dolomitic limestone. The base of the formation is marked by the change from the hard dolomitic limestone of the Hummar Formation which forms together with lower part of Shuayb a prominent cliff. The top is defined by a sudden change from gentle slopes to hard, thick-bedded and then to the massive dolomite and dolomitic limestone of Wadi Es Sir Limestone Formation which form prominent cliffs and steep slopes. The Shuayb Formation was deposited in the Early Turonian in a moderate to shallow subtidal marine environment (Powell, 1989).

2.1.1.2. Wadi Es Sir Limestone Formation

The formation consists of three distinctive units. The lower part is comprised of dolomite, dolomitic limestone, the middle part consists of soft marly limestone and limestone, and the upper unit consists almost totally of thick-bedded to massive limestone. The thick-bedded to massive limestone of the formation forms distinctive rocky steep slopes. The formation was deposited on a wide shallow marine carbonate platform

within tidal to lagoon regimes. The formation marks the maximum extent of the marine transgress pulses during the Cenomanian to the late Turonian- middle Coniacian time (Abed, 2000).

2.1.2. Belqa Group

2.1.2.1. Wadi Umm Ghudran Formation

The best section of this formation is provided by the road-cut on the Irbid-Jarash road 0.5 km south east of Balila. The lower half consists of 15~m of yellow to white gray; locally pink gray, and buff, reworked, fragmental and fossiliferous chalky limestone which marks the unconformity with the underlying Ajlun Group. The upper half consists of about 15m of limestone and chalky limestone typically pink to yellow grey, hard, medium, to thin-bedded, fossiliferous to coquinal, and with chert concretions and bands toward the top, alternating with yellow to white grey, medium-bedded and soft chalk marl. The formation was deposited in a moderate to a deep- water pelagic environment during the late Coniacian to the Santonian time (Abdelhamid, 1995).

2.1.2.2. Amman Silicified Limestone Formation

The formation consists of dark brown to grey thick-bedded chert, phosphatic chert, silicified limestone, marl, siliceous coquina and brecciated chert which were formed in a shallow-marine environment during Santonian to Campanian (Abed, 2000).

2.1. Tectonic Setting

The study area is located to the east of the Dead Sea Transform (DST) (Figure 1). The DST separates the Arabian and Sinai-Palestine sub- plates, and connects the Red Sea in the south with the collision belt of southern Turkey. The Dead Sea Transform is left lateral, and is comprised of a zone of en-echelon strike-slip faults. Motion on the (DST) initiated in the Miocene and has a cumulated lateral displacement of about 105 km (e.g. Quennell, 1951; Quennell, 1983; Freund et al., 1970; Garfunkel, 1981). Geological observations indicate that two distinct paleostress regimes operated adjacent to the Dead Sea rift: 1) WNW- shortening and NNE- extension, beginning in the Turonian and associated with the development of the Syrian Arc fold belt and is attributed to the Syrian Arc Stress field (SAS). 2) Middle Miocene to recent NNW shortening and ENE extension, associated with the 105- km sinistral displacement along the Dead Sea Transform and the opening of the Red Sea, and is attributed to the Dead Sea stress field (DSS) (Eyal, 1996; Diabat et al., 2004). The concurrent development of the DST system has resulted in a complex tectonic history that has led to several phases of deformation in the relatively young Upper Cretaceous rocks (Eyal, 1996).

3. Methodology

This research depends essentially on field investigations. The methods of investigation include the following integrated components:

- The scanline method involves laying a tape along the length of an outcrop determining its orientation. Then, the position along it where each fracture intersects the tape, the orientation, length of the fracture, and the type of fracture are recorded.
- The Circle-Window method involves drawing a circle on the outcrop that encompasses at least thirty different fractures to make sure that the results are unbiased and statistically significant. Once the circle is on the outcrop, one counts the number of fractures that intersect the circle and the number of fractures that terminate within the circle. These two measurements provide an accurate density and intensity of the fractures.
- The Common method involves measuring a random-fracture orientation.

The specific locations were chosen to allow the determination of the change in density and intensity of the fractures nearing different structural features, such as faults and shear zones, and on differently-oriented surfaces, for

instance horizontal and vertical surfaces, that were near each other.

Nine stations were selected which represented different parts of the study area. In the circle method, a circle of a known as well as a predetermined radius is traced on the surface hosting fracture; in this case, it was a bedding plane all the time and it requires measuring all the fractures occupied by the circle. The orientation, length, and width of each fracture within the circle were measured. Circles, having a radius of 3.5 m at least were traced out on the bedding plane by the help of chalk and a measuring tape; orientation of fractures were measured in terms of strike; length and width were measured by the help of a simple ruler and a measuring tape. To avoid repetition, each fracture was traced with chalk after the measurement. As for measuring orientation, only traces of the straight lines of the fractures were evident at the bedding plane and because of that only strikes of the fractures were measured.

4. Results

The study area has been sub-divided into nine main stations, namely along the Irbid- Jerash Highway; in abandoned quarries, and road-cuts. Table (1) and figure (2) show the location and type of structures that have been investigated in each station.

Table 1. Location, measurements and fractures density (f/m) of the stations in the study area.

Station No.	Coordinates	No. of data	Type of structures	Measuring method	Scanline method (f/m)	Circle method (f/m)
1	32° 22.633' N 35° 56.268' E	100	Fractures (joints, and faults)	Common	-	-
2	32° 22.425' N 35° 55.890' E	90	Joints, faults, and bedding planes	Scanline /common	7.8	-
3	32° 22.016' N 35 ° 55.592' E	118	joints/bedding planes	scanline /common	14.8	-
4	32° 21.780' N 35° 55.319' E	231	Fractures (joints, strike-slip faults)	common/ circle / scanline	5.1	5.8
5	32° 21.701' N 35° 55.223' E	312	Fractures (joints, strike-slip faults)	Common/ circle /scanline	6.3	1.7
6	32° 21.701' N 35° 55.223' E	79	Fractures, normal faults, thrust faults, strike slip faults	common /scanline	7.9	-
7	32° 19.674' N 35° 56.085' E	387	Fractures (joints, strike-slip faults), bedding planes	common /circle /scanline	6.2	8.1
8	32° 19.305' N 35° 55.147' E	37	Fractures (joints, normal faults, strike-slip faults)	common/ scanline	5.75	-
9	32° 21.229' N 35° 54.348' E	31	joints, strike-slip faults	common / scanline	4.7	-

Orientation data were collected from the Wadi Es Sir Limestone Formation (Turonian) (Figure 2). The sections consist of limestone beds, interlayer with marlstone and chalky limestone, and vary in thickness at different places. The majority of rocks are highly-fractured. The fractures encountered in the study area are either extensional spanning

numerous beds, or are constructed in a defined layer. Joint orientations continued from one to three joint sets in each station. The majority of joints have surface structures such as the plumose structure or mineralization. More than 70 throughgoing fractures were measured in the study area; they exhibit a wide range of geometries and dimensions.

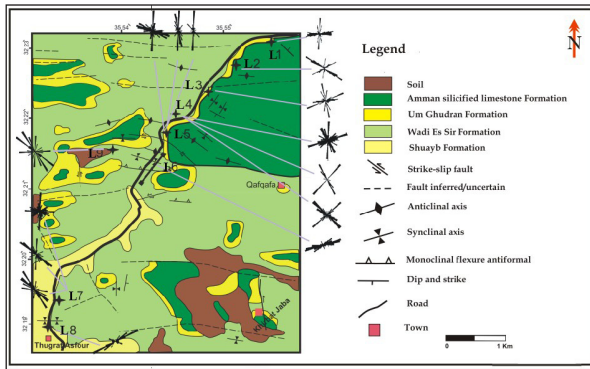


Figure 2. Geological map with displayed trends of measured structures in each station.

All throughgoing fractures are steeply dipping to vertical, and despite the considerable scattering in orientation, they reveal dominant ENE- WSW, NW-SE and N-S trends. Many extensional fractures have been filled with calcite.

Bedding plane orientations that have been measured along road-cuts and other places show a gentle dip (<15°). Faults encountered in the study area include the three main types (normal, reverse and strike-slip). The most abundant is the strike- slip with a ratio of 70%. At less amounts, the normal faults are distributed in many stations especially road cuts, forming small horsts and grabens, and listric structures.

The data for each station were plotted using stereographic projection and rose diagrams. The geological map of the study area is shown in figure (2) with the detailed structural features and rose diagrams.

Station 1

One-hundred measurements were taken from an abandoned quarry located at the eastern side of the Irbid-Jerash road (Figure 2 and Table 1). The measurements included joints and strike-slip faults. Two main set trends were observed; N-S and E-W.

Some of these fractures are confined to specific beds and others are throughgoing. Slickenlines appear clearly on the fault planes that indicate the movement direction.

Station 2

Ninety measurements were taken from road cuts at the eastern side of the Irbid- Jarash road (Table 1 and Figure 2). Measurements include bedding planes, joints, and small faults. Bedding plane orientations have been measured forming an anticline slightly plunging toward NNW (Figure 3). Fracture planes are vertical to sub-vertical and have a main trend oriented NW-SE and two minor trends oriented NNE-SSW and NE-SW. The majority of fractures are confined to the bedding and show a high density forming swarms of closely-spaced joints (5cm). Fractures were measured using the scanline method and other common methods (Table 1) (Figures 4 - 5):

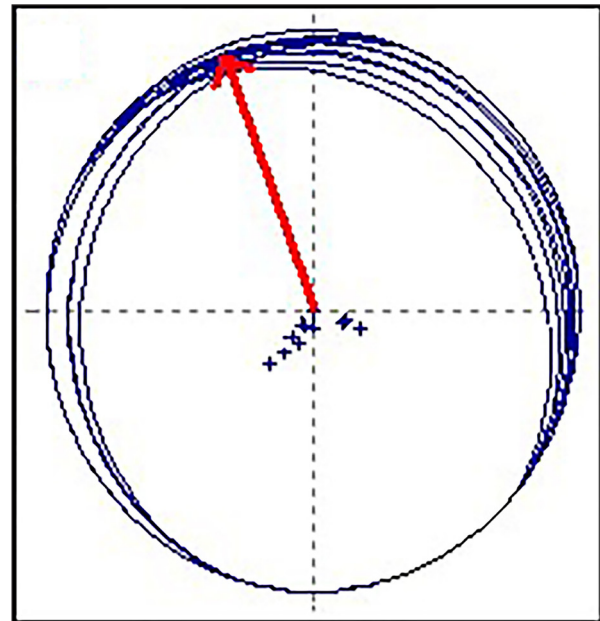


Figure 3. Stereoplote of local slightly plunging anticline towards NNW.

The red arrow is the plunge direction; the great circles are the bedding planes; while crosses are the poles to bedding planes.



Figure 4. Fracture swarms of closely-spaced extensional to hybrid fractures. Tr.1 and Tr. 2 represent the number of measured fractures.

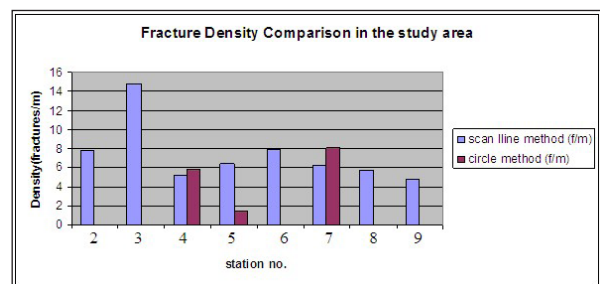


Figure 5. Histogram represents fractures density in each station.

Many structures can be traced along the road cut; a positive flower structure occurred as a consequence of the compressive stresses affecting the stratigraphic layering.

A fault zone spanning the entire exposure was observed at the road cut. The zone of deformation is characterized by the presence of gouge, crushed rocks, and a dragging of strata.

Station 3

One-hundred and eighteen measurements were taken from a quarry at the eastern side of the Irbid- Jerash road using scanline and common methods (Table 1 and Figure 3). Rocks are highly deformed forming a gentle anticline plunging to NNE (Figure 6). Joints show two main set trends ENE-WSW and NNW-SSE. Fractures in most cases are aligned in a vertical sequence. A major multilayer dextral fault was encountered in this station striking E-W and dipping 60° toward the south (Figure 7). The fault plane is highly polished and the rocks adjacent to the fault zone are highly deformed, tilted, and brecciated.

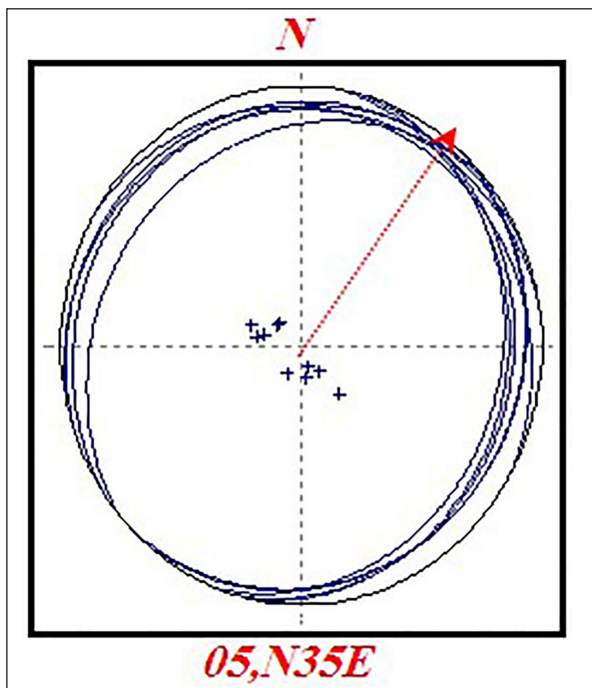


Figure 6. Stereoplot of a gently plunging anticline. The number and arrow in red color is the plunge and plunge direction (05/ N35E) of the anticline; crosses are poles to bedding planes.

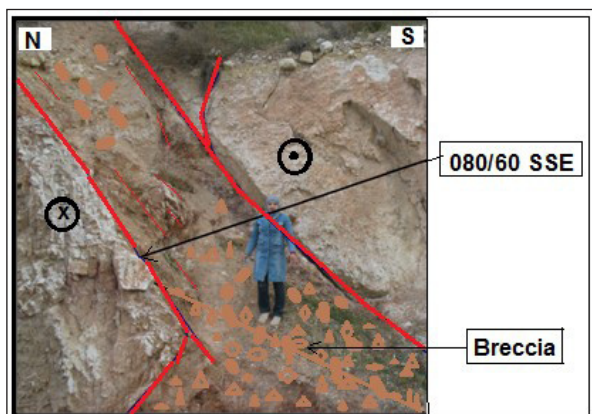


Figure 7. A dextral fault zone cut across the dipping strata.

Station 4

Two-hundred and thirty-one fracture measurements were taken from a quarry at the western side of the Irbid-Jerash road (Table 1 and Figure 2). Fractures density has been calculated using scanline, circle, and common methods

(Table 1). Two main fracture sets oriented ENE-WSW, N-S and two minor sets oriented NNW-SSE, NW-SE were observed. Joints are steeply dipping, aligned in a vertical to a sub-vertical sequence. The investigated fractures are grouped into two main types due to their development (according to Gross and Eyal, 2007):

Bed-confined joints: which are confined to individual beds (unmineralized joints) and are closely-spaced.

Multilayer joints that cut across numerous beds (throughgoing fractures) that developed subsequent to the bed-confined joints. They commonly form by coalescence (linkage and preferential widening) of preexisting joints. They are grouped into three main categories based on their geometries;

- a. Incipient: steeply dipping, sub-parallel fracture segments consisting of slightly widened and bed-confined cross joints.
- b. Linked throughgoing fracture: continuously connected from their lower to upper tips, and in some cases are composed of numerous, vertically-aligned cross joints linked together across stratigraphic intervals by short segments consisting of bed-parallel and shallow-dipping fractures resulting in a zigzag geometry.
- c. Throughgoing fractures with aperture: they are linked structures that have developed significant mechanical aperture (>0.5cm) across the majority of opposing segment walls. The apertures reflect dominantly an opening mode of displacement.

Slickenlines are preserved on fault surfaces serving as excellent kinematic indicators of a strike-slip motion (Figure 8). Plumose structures are formed on joint surfaces to represent the point at which the joint started to grow representing the inhomogeneous behavior in rocks when subjected to stress.



Figure 8. Slickenlines with calcite steps as a sense of movement indicator of sinistral strike-slip fault, in which the missing plane moved in the direction of the blue arrow.

Station 5

Three-hundred and twelve fracture measurements were taken from a quarry at the eastern side of the Irbid- Jerash road (Table 1 and Figure 2). Circle and scanline methods were also applied in this station to compare the fractures' density with the other stations (Table 1). Joints' orientation is grouped into two trends; N-S and WNW-ESE. Many joints aligned in vertical to sub-vertical planes. Other throughgoing joint sets have a parallel trend and are oriented NNW. Joints were enlarged by water solutions forming small cavities (Figure 9). Many throughgoing fractures are linked along the sequence and others are filled with calcite.



Figure 9. Systematic throughgoing fractures enlarged by solutions.

Station 6

Seventy-nine fracture planes were taken at the eastern side of the Irbid-Jerash road cut using scanline method (Table 1 and Figure 3). The main fracture set trend is oriented ENE- WSW and a minor set is oriented NNW-SSE. The characteristic feature along the road cut is the presence of many types of mesostructures e.g. local folds, the high density of normal faults forming horsts and grabens.

Most of normal faults were observed in this station along the road cut. Their geometries vary from short to multilayers that span the entire exposure. These faults cluster into two populations based on orientation, forming a conjugated system with a mean dip of (60° - 75°), and the majority of these faults strike NW-SE.

Special structural features were observed in the rock layers in this station including the boudinage structure (Figure 10). Dipping strata are highly-faulted by reverse faults and thrust faults forming wedge-thrust faults (Figure 11). They are curved and accompanied by folding and uplift depending on the direction of curvature with respect to the sense of displacement.



Figure 10. Boudinage structure formed due to the competent and incompetent contrast layers.

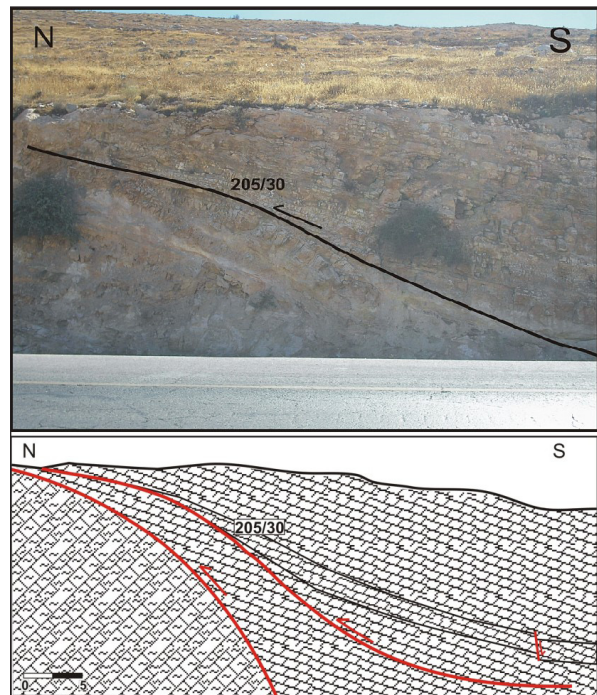


Figure 11. Photo and sketch cross- section showing a wedge thrust fault which resulted from local north-south compression.

Station 7

Three-hundred and eighty-seven measurements were recorded for joints in this quarry in the southern part of the study area at the eastern side of the Irbid-Jerash road (Figure 2). Three methods of data collection were applied in this station (Table 1). A comparison with the other quarries was made using the circle method and scanline to conclude the intensity of fractures in each quarry (Table 1). Joints oriented into two main trends; N-S and E-W. Many joints terminate at bed boundaries (bed-confined) displaying regular spacing and are vertically aligned. Other fractures cut across the whole exposure forming linked throughgoing fractures, throughgoing fractures with aperture and in the late phase of development and those of the opening mode that are filled with calcite (Figs. 12 - 13). Many slickenlines served on the fault surface to indicate the strike-slip or oblique motion. Fault surfaces in general have a vertical alignment trending

E-W and some of them have been karstified. Layers slightly dip (20°) toward the south east.



Figure 12. Karstified throughgoing fracture filled with calcite.

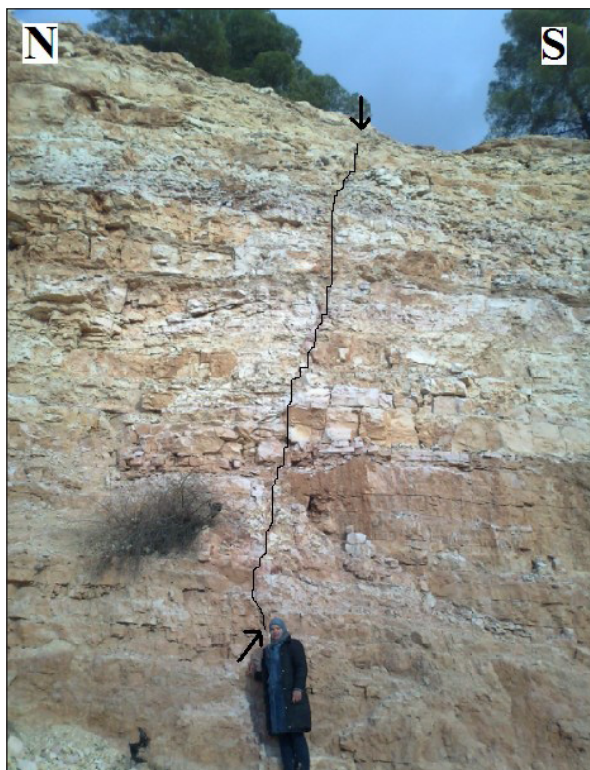


Figure 13. Single linked throughgoing fracture.

Station 8

Thirty-seven joint measurements were taken from this station in the southern part of the study area at the western

side of the Irbid- Jerash road (Table 1 and Figure 3). The fractures show a main set trend ENE-WSW and minor set trends in ESE-WNW extending vertically along the bed sequence. Fractures density increase within and near fault zones. The scanline method was applied on fractures (Figure 14) and fracture density has been calculated.

Rock layers that are highly deformed resulting in many structures were observed on the road cut. Negative flower structures developed on which the slip on subsidiary faults had a normal sense component in transtensional zones within strike-slip systems. Listric faults which occurred when fault surfaces in some cases are not planar (Figure 15) were observed. Slickenlines on fault planes that indicate the strike-slip and oblique movements were also observed.

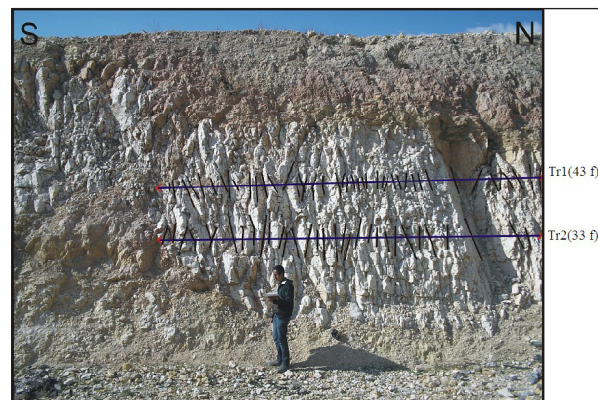


Figure 14. Fracture swarm's density using scanline method. Tr1 (43 f) and Tr2 (33 f) represent the number of measured fractures along traverses.

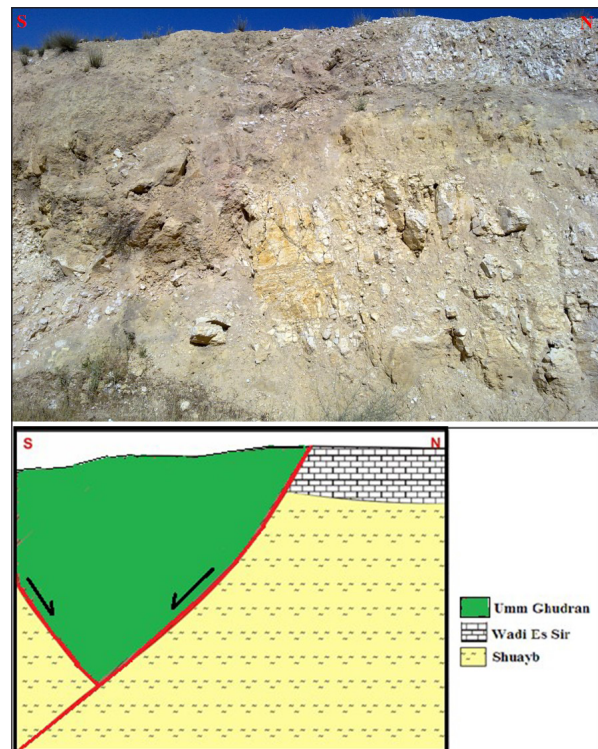


Figure 15. A photograph and sketch cross section showing a negative flower structure.

Station 9

This station includes three neighboring quarries located at the western side of the Irbid-Jerash highway (Figure 2). Measurements were taken for both fractures and bedding planes (Table 1). The orientations of bedding planes were measured; the dip is 20° toward 170° . Fractures of both types were encountered including throughgoing and bed-confined fractures. Fractures are aligned sub-vertically to vertically along the stratigraphic layering, some of them are dipping 60° . In addition, many slickensides and slickolites were encountered serving on fault planes which indicate the strike-slip motion. The orientation of slickensides on the fault planes was measured; the movement was very clear and the rocks were highly deformed within the fault zones which formed the fault breccia consisting of limestone and chert fragments. A small normal fault was observed in the stratigraphic layering but in limited extension, the apparent down throw does not exceed 30-40 cm (Figure 16).



Figure 16. A small normal fault with down throw (20 cm).

5. Discussion

The present study reveals meso-scale structural features throughout the Upper Cretaceous rocks. These features mostly affected the hard limestone units of Wadi Es Sir Limestone Formation and can be classified as compressional or extensional structures.

The compressional structures are folds, thrust reverse faults, positive flower structure and stylolites. The extensional structures are normal faults and their associated structures include horsts and grabens, listric faults, negative flower structure, boudinage structure, joints and veins. Axes of boudinage are arranged in a nearly E-W direction. Boudinage and pull-apart structures are an expression of local layer-parallel extension, and are often laterally replaced by small-scale thrusts and asymmetric small-scale folds in the same layer in the area of the local layer-parallel contraction (station 6). Rock layers are highly-deformed resulting in many structures that were observed on the road cut including negative flower structures which

developed where the slip on subsidiary faults had a normal sense component in transtensional zones within strike-slip systems, and listric faults.

In general, fractures were traced intensively all through the study area, and more than 1385 fracture measurements were collected a long road cuts and quarries. The field work reveals that fractures are concentrated in high densities throughout the study area and are oriented in many trends, but in most cases, in zones of deformation (such as fault zones) and fold crests as can be seen along the road cuts in stations (2, 3 and 6).

The major trends NW-SE, NNW-SSE and N-S with other minor trends, ENE-WSW and E-W dominate the study area. The number of joint sets at each station is variable ranging from one set (e.g., stations 6 and 8) to four sets (e.g. station 4). This is due to the local variation of structural position.

To interpret the results easily, rose diagrams for each station were displayed on the geological map (Figure 2). Orientation of all fractures are represented as rose diagrams (Figure 17). All measured strike-slip faults, normal faults, throughgoing fractures, and slickenlines in the study area were also represented separately as rose diagrams and/or stereoplots (Figure 17).

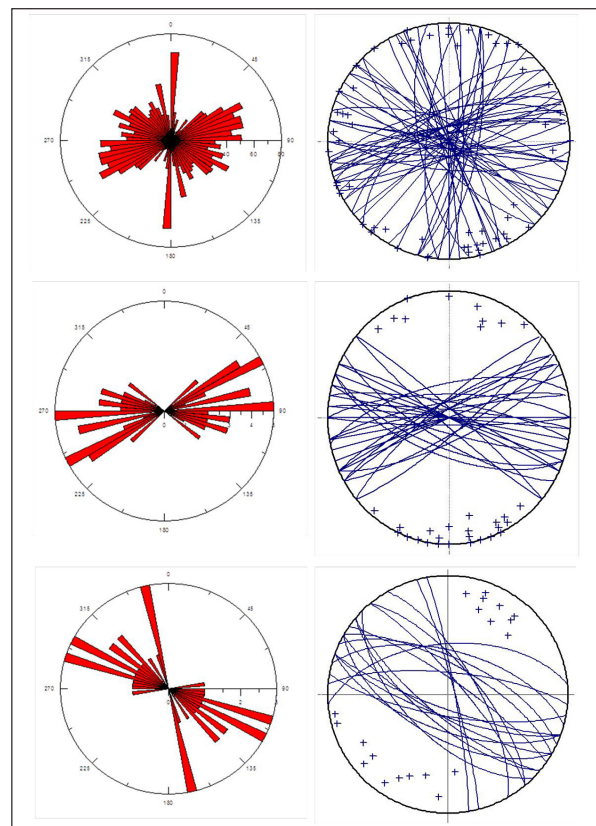


Figure 17. a) Rose diagram and stereoplot of fracture orientation of all stations in the study area. b) Rose diagram and stereoplot of all throughgoing fractures in the study area. c and d) Rose diagram and stereoplot show the orientation of all strike-slip faults in the study area. e and f) Rose diagram and stereoplot of all normal faults in the study area.

Figures (2 and 18) show two dominated trend sets of fractures oriented N-S and NNW to NW in addition to other minor trend sets in E-W, ENE- WSW and WNW-ESE. The N-S and NNW to NW dominant trends represent the range of conjugated, hybrid and extensional fractures.

The ENE-WSW to E-W trend set of figures (2, 17 a) reflects the majority of fault-slip data analyzed. Plane surfaces of these fractures are mainly coated with calcite steps or slickolites which are of importance as a sense movement indicator, the plunge and azimuth of these structural markings were measured. Investigations show that dextral shear along these fractures have occurred later as a reactivation process. These fault planes are open and calcite curtains or soil staining on their surfaces (Diabat, 2013). Figure (17b) shows no preferred orientation of the throughgoing fractures in the study area, which can be explained as brittle deformation progress. It was more efficient for throughgoing fractures to utilize (reactivate) preexisting fractures rather than to propagate new fracture surfaces in intact rock. This means that they could take the orientation of any preexisting fractures in the study area. Many throughgoing fractures develop subsequent to bed-confined joints, for thin- to medium- bedded rocks, where bed-confined fractures are closely spaced throughgoing fractures are commonly formed by the coalescence of pre-existing joints. Structural geometries indicate a clear temporal order in the formation of the three main fracture populations. Throughgoing fractures were then formed by the coalescence and linkage of selective zones of vertically aligned, preexisting, bed-confined joints. In station 6, there is a contractional tectonic setting, in which the assemblage in the thrust-fold zone indicates that there was a layer-parallel shortening normal to the fold hinge line or axial elongation deformation occurring in a contractional environment. The extensional faults and allied structures in this zone (e.g. boudins) are interpreted as a local product of stretched fold limbs.

6. Conclusions

- Fractures are concentrated in high densities throughout the study area, and are oriented in many trends in most cases, in zones of deformation like fault zones and fold crests as can be seen along the road cuts in stations (2, 3, and 6).
- Many throughgoing fractures develop subsequent to bed-confined joints by the coalescence of pre-existing joints.
- Many joints aligned in vertical to sub-vertical planes. Other throughgoing joint sets are of a parallel trend and are oriented NNW. Joints were enlarged by water solutions forming small cavities.
- The normal fault systems that formed horsts and grabens are thought to be conjugated.
- Many slickensides and slickolites served on fault planes indicate the strike-slip motion.
- This study shows two dominated trend sets of fractures oriented N-S and NNW to NW in addition to other minor

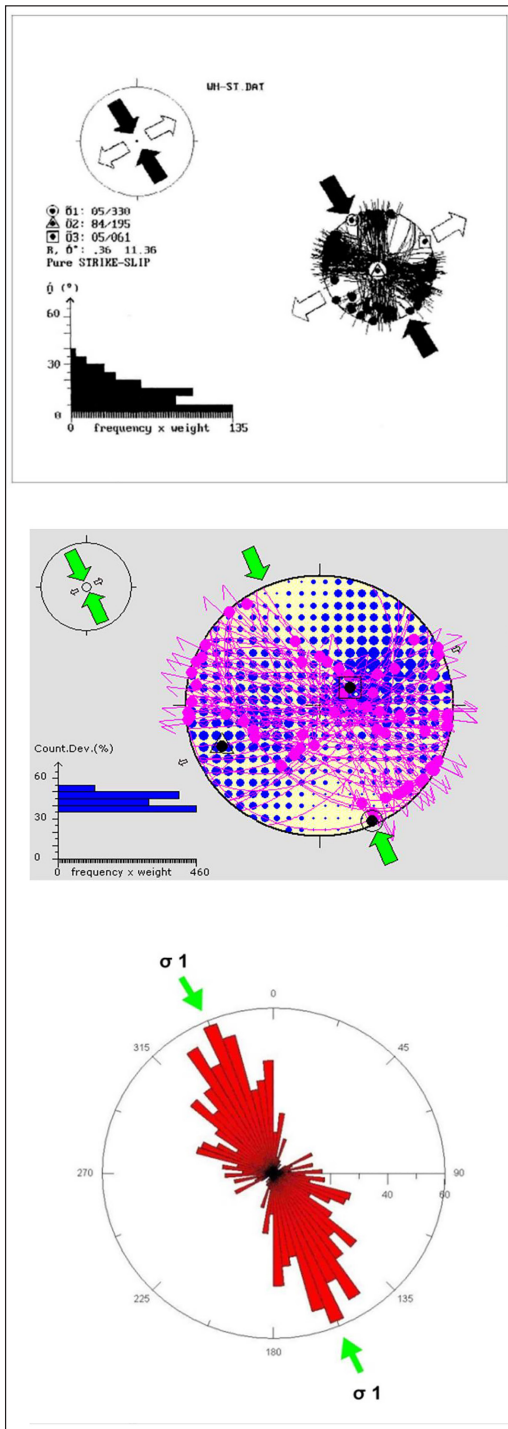


Figure 18. a) Principal stress axes determination by using the TENSOR program and fault-slip data along the Dead Sea transform (DST); inward arrows indicate compression (σ_1), outward arrows indicate tension (σ_3), whereas σ_2 is vertical (Diabat, 1999; Diabat et al., 2004). b) Principal stress axes of 70 fault-slip measurements in northern Jordan; outward ENE arrows indicate tension (σ_3) and inward NNW arrows indicate compression (σ_1), σ_2 is vertical (Diabat, 2013). c) Strike of 740 fracture planes and the deduced SH_{max} from the orientation of extensional fractures in northern Jordan (Diabat, 2013).

trend sets in E-W, ENE- WSW and WNW-ESE.

References

- Abdelhamid, G.H. (1995). The geology of Jarash Area Map Sheet (3154-I), Report of Natural Resource Authority. Geology Directorate, Natural Resources Authority (Ministry of Energy and Mineral Resources) Amman, Jordan.
- Abed, A.M. (2000). Geology of Jordan, 1st edition. Jordanian Geologists Association. (In Arabic).
- Al-Awabdeh, M., Perez-Pena, J.V., Azanon, J.M., Booth-Rea, G., Abed, A., Atallah, M., Galve, J.P. (2016). Quaternary tectonic activity in NW Jordan: Insights for a new model of transpression–transtension along the southern Dead Sea Transform Fault. *Tectonophysics* 693: 465-473.
- Al-Taj, M., Atallah, M., Abed, A. (2003). Fractures Associated with the Dead Sea Transform in the Jordan Valley, Jordan. *Abhath Al – Yarmouk, Series of Basic Sciences and Engineering* 12(2B): 633-647.
- Atallah, M. (1996). Joint and fault analysis in Al-Husn fold belt - northern Jordan. *Abhath Al-Yarmouk, Series of Basic Sciences and Engineering* 5: 187-201.
- Davis, G.H., Reynolds, S.J., Kluth, C.F. (2011). *Structural Geology of Rocks and Regions*. 3rd edition. New York, John Wiley and Sons. 864 P.
- Diabat, A. (1999). Paleostress and strain analysis of the Cretaceous rocks in the eastern margin of the Dead Sea transform, Jordan. Ph.D Thesis, University of Baghdad.
- Diabat, A. (2009). Structural and stress analysis based on fault-slip data in the Amman area, Jordan. *Journal of African Earth Sciences* 54: 155-162.
- Diabat, A. (2013). Fracture systems and dissolution cavities development in hard carbonates, northern Jordan. *Jordan Journal of Earth and Environmental Sciences* 5 (2): 73-78.
- Diabat, A. and Masri, A. (2005). Orientation of the principal stresses along Zerqa- Ma'in Fault. *Mu'ta Lil-Buhuth Wad-Dirasat* 20: 57- 71.
- Diabat, A., Atallah, M., Salih, M.R. (2004). Paleostress analysis of the Cretaceous rocks in the eastern margin of the Dead Sea transform, Jordan. *Journal of African Earth Sciences* 38: 449-460.
- Eyal, Y. (1996). Stress fluctuations along the Dead Sea rift since the Middle Miocene. *Tectonics* 15: 157-170.
- Eyal, Y. and Reches, Z. (1983). Tectonic analysis of the Dead Sea rift region since the Late Cretaceous based on Mesostructures. *Tectonics* 2:167-185.
- Eyal, Y. Gross, M.R. Engelder T., Becker A. (2001). Joint development during fluctuation of the regional stress field in Southern Israel. *Journal of Structural Geology* 23: 279-269.
- Freund, R., Garfunkel, Z., Zak, I., Goldberg, M., Weissbrod, T., Derin, B. (1970). The shear along the Dead Sea rift. *Philosophical Transaction of the Royal Society of London* 267: 107- 130.
- Garfunkel, Z. (1981). Internal structure of the Dead Sea leaky transform (rift) in relation to plate kinematics. *Tectonophysics* 80: 81– 108.
- Gross, M.R. and Eyal, Y. (2007). Throughgoing fractures in layered carbonate rocks. *Geological Society of America Bulletin* 119: 1387-1404.
- Hancock, P.L. (1985). Brittle microtectonics: Principles and Practices. *Journal of structural Geology* 7: 347 - 457.
- Hancock, P.L. and Atiya, M.S. (1979). Tectonic significance of the mesofracture systems associated with the Lebanese segment of the Dead Sea transform fault. *Journal of Structural Geology* 1: 143-153.
- Powell, J.H. (1989). Stratigraphy and sedimentation of the Phanerozoic rocks in central and southern Jordan. *Bulletin 11, Geology Directorate, Natural Resources Authority (Ministry of Energy and Mineral Resources) Amman, Jordan. Part B: Kurnub, Ajlun and Belqa Groups*. 161 p.
- Quennell, A.M. (1951). The Geology and mineral resources of former Transjordan. *Colon Geol Min, Resource* 2: 85-115, London.
- Quennell, A.M. (1983). Evolution of the Dead Sea Rift. A review, *First Jordanian Geologic Conference*, 460-482.
- Radaideh, O.M. and Melichar, R. (2015). Tectonic paleostress fields in the southwestern part of Jordan: New insights from the fault slip data in the southeastern flank of the Dead Sea Fault Zone. *Tectonics* 34 (9): 1863-1891.